VIMS Articles   Virginia Institute of Marine Science

2015

Characterization and comparison of toxin-producing isolates of Dinophysis acuminata from New England and Canada

MM Tong

Juliette L. Smith
Virginia Institute of Marine Science

M Richlen

KA Steidinger

DM Kulis

See next page for additional authors

Recommended Citation

Authors

MM Tong, Juliette L. Smith, M Richlen, KA Steidinger, DM Kulis, and Et al.

Characterization and comparison of toxin-producing isolates of *Dinophysis acuminate* from New England and Canada[1]

Mengmeng Tong,
Ocean College, Zhejiang University, Hangzhou, 310058, China

Woods Hole Oceanographic Institution, Biology Department and the Woods Hole Center for Oceans and Human Health Woods Hole, Massachusetts, 02543, USA

Juliette L. Smith,
Woods Hole Oceanographic Institution, Biology Department and the Woods Hole Center for Oceans and Human Health Woods Hole, Massachusetts, 02543, USA

Virginia Institute of Marine Science, College of William and Mary, Gloucester Point, Virginia, 23062, USA

Mindy Richlen,
Woods Hole Oceanographic Institution, Biology Department and the Woods Hole Center for Oceans and Human Health Woods Hole, Massachusetts, 02543, USA

Karen A. Steidinger,
Florida Fish and Wildlife Conservation Commission, Fish and Wildlife Research Institute, St Petersburg, Florida 33701, USA

David M. Kulis,
Woods Hole Oceanographic Institution, Biology Department and the Woods Hole Center for Oceans and Human Health Woods Hole, Massachusetts, 02543, USA

Elie Fux, and
U.S. FDA, Division of Seafood Science and Technology, Dauphin Island, Alabama 36528, USA

Donald M. Anderson
Woods Hole Oceanographic Institution, Biology Department and the Woods Hole Center for Oceans and Human Health Woods Hole, Massachusetts, 02543, USA

Abstract

Following the identification of the first toxic isolate of *Dinophysis acuminata* from the northwestern Atlantic, we conducted detailed investigations into the morphology, phylogeny, physiology, and toxigenicity of three isolates from three sites within the northeastern U.S./Canada region: Eel Pond and Martha's Vineyard, Massachusetts, and the Bay of Fundy. Another isolate, collected from the Gulf of Mexico, was grown under the same light, temperature, and prey conditions for comparison. Despite observed phenotypic heterogeneity, morphometrics and molecular evidence classified the three northwestern Atlantic isolates as *Dinophysis acuminata*

Claparède & Lachmann, whereas the isolate from the Gulf of Mexico was morphologically identified as *D.* cf. *ovum*. Physiological and toxin analyses supported these classifications, with the three northwestern Atlantic isolates being more similar to each other with respect to growth rate, toxin profile, and diarrhetic shellfish poisoning (DSP) toxin content (okadaic acid + dinophysistoxin 1/cell) than they were to the isolate from the Gulf of Mexico, which had toxin profiles similar to those published for *D.* cf. *ovum* F. Schütt. The DSP toxin content, 0.01 – 1.8 pg okadaic acid (OA) + dinophysistoxin (DTX1) · cell^{-1}, of the three northwestern Atlantic isolates was low relative to other *D. acuminata* strains from elsewhere in the world, consistent with the relative scarcity of shellfish harvesting closures due to DSP toxins in the northeastern U.S. and Canada. If this pattern is repeated with analyses of more geographically and temporally dispersed isolates from the region, it would appear that the risk of significant DSP toxin outbreaks in the northwestern Atlantic is low to moderate. Finally, the morphological, physiological, and toxicological variability within *D. acuminata* may reflect spatial (and/or temporal) population structure, and suggests that sub-specific resolution may be helpful in characterizing bloom dynamics and predicting toxicity.

Keywords

Dinophysis acuminata; *Dinophysis acuminata* complex; morphology; *cox*1; peduncle; Diarrhetic Shellfish Poisoning; okadaic acid; pectenotoxins

Introduction

The dinoflagellate genus *Dinophysis* comprises over 75 species (Gómez 2012), 10 of which are known to produce okadaic acid (OA) and its derivatives associated with diarrhetic shellfish poisoning (DSP; Wilkerson and Grunseich 1990, FAO 2004, Johnson 2011, Reguera et al. 2012, Reguera et al. 2014). A closely related genus, *Phalacroma*, contains about 70 heterotrophic species of which two are listed as producing toxins, although the toxin content of cells may be due to phagotrophy of toxic prey. These toxins can accumulate in filter-feeders, such as bivalve shellfish, and adversely affect human and other animal consumers. In humans, the symptoms of DSP include diarrhea, nausea, vomiting, and abdominal pain. Pectenotoxins (PTXs) are commonly quantified and reported along with DSP toxins, as they are usually co-produced within the same organisms, but diarrhea was not observed in mice administered PTXs (Miles et al. 2004b). The mode of action for PTXs is still under investigation.

Harmful algal bloom (HAB) monitoring programs in coastal U.S. waters rely on testing for toxins in shellfish meat and, in some regions, additional microscopic identification of toxic or potentially toxic harmful algae species in proximity to shellfish growing areas or aquaculture sites. Positive results from the latter can prompt more intensive monitoring of both the plankton and shellfish, which in turn can lead to closure of harvesting areas to protect public health. In the northern U.S., toxic dinophysoid species are usually represented by members of the *Dinophysis "acuminata"* complex (e.g., *D. acuminata* Claparède & Lachmann, *D. saccula* Stein, *D. ovum* Schütt), but *D. acuta* Ehrenherg, *D. caudata* Saville-

Kent, *D. fortii* Pavillard, *D. norvegica* Claparède & Lachmann and *D. tripos* Gourret have also been reported in the region (Hargraves and Maranda 2002).

Microscopic identification of *Dinophysis* spp. involves characteristics such as cell contour and sulcal lists (Larsen and Moestrup 1992); however, gradation between certain character traits of the species, angle of observation of individual cells, and existence of different life stages, make it difficult to differentiate cells as *D. acuminata* or *D. ovum* (Reguera and Gonzalez-Gil 2001, Escalera and Reguera 2008, Reguera and Pizarro 2008). Therefore, some of the distinct morphotypes of this species complex have been referred to as *D. acuminata*, *D.* cf. *acuminata*, *D. ovum*, and *D.* cf. *ovum* on the basis of their oval/suboval shape in lateral view and the dorsal convexity of the hypothecal plates (Reguera et al. 2012).

Molecular methods have been developed to identify many dinoflagellate species and clades, but the taxonomic assignment of *Dinophysis* species using molecular characters is still unresolved due to extremely low interspecific variability within their nuclear ribosomal genes and intergenic regions, the typical targets of such studies (Raho et al. 2013). Phylogenetic analysis of large subunit ribosomal DNA (LSU rDNA) sequences identified two major clades of photosynthetic *Dinophysis*, but could not discriminate among *Dinophysis acuminata*, *Dinophysis dens* Pavillard, *Dinophysis saccula*, and *Dinophysis acuta* (Edvardsen et al., 2003). Internal transcribed spacer (ITS) regions also had low resolving power, and exhibited a 99% similarity between *D. acuminata* and *D. saccula* (Marin et al. 2001). The mitochondrial cytochrome c oxidase (mt *cox1*) gene may be a suitable marker for examining the taxonomy of *Dinophysis*, as it was used to distinguish two morphologically similar species of the "*Dinophysis acuminata* complex" – *D. acuminata* and *D. ovum* – from Galicia (northwest Spain; Raho et al. 2008). However, more recent work by Raho et al. (2013) found that neither mt *cox1* nor cytochrome b (cob) genes provided sufficient resolution to identify six *Dinophysis* species (field isolates and cultures of *Dinophysis tripos* Gourett, *Dinophysis caudata* Saville-Kent and *Dinophysis saccula*).

Species in the *"acuminata* complex" have been reported from coastal waters of the northwestern Atlantic, the region of focus here, and although these species are toxic in other parts of the world, no DSP incidents conclusively linked to *Dinophysis* spp. have been reported in this region. Previous work confirmed that local isolates of *Dinophysis* from Eel Pond, (Woods Hole MA, U.S.) were *D. acuminata*, producing OA, OA-D8 (diol ester of OA), DTX1 and PTX2 (Hackett et al. 2009, Fux et al. 2011, Tong et al. 2011) in monoculture. Other work (Smith, unpublished data) has shown that dissolved DSP toxins are present in the region's coastal waters. Hattenrath-Lehmann et al. (2013) documented the first occurrence of DSP toxins in shellfish exceeding the U.S. FDA action level (i.e., 16 µg [(OA) + DTXs] · 100 g^{-1} edible shellfish tissue) in the region, Northport Bay, NY. Within the U.S., only *Dinophysis* cf. *ovum* (Gulf of Mexico; Campbell et al. 2010) and *D. acuminata* (Washington state, Trainer et al. 2013, New York, Hattenrath-Lehmann et al. 2013) have been linked to closures of shellfish harvesting due to DSP toxins measured above guideline levels in shellfish. A closure precipitated by high cell densities of *D. acuminata* in the Chesapeake Bay only revealed trace quantities of DSP toxins in plankton and shellfish samples (Tango et al. 2002).

Given the widespread presence of toxic *D. acuminata* and other *Dinophysis* species in the northeastern region of the U.S. and Canada, but the general lack of reports of hazardous levels of toxins in shellfish from the region, the objective of this work was to characterize and compare multiple *Dinophysis* isolates from the northwestern Atlantic to better understand the region's species heterogeneity and potential for toxicity. To fully characterize the region's isolates, cultures were grown under similar light, temperature and prey conditions, and their morphology, phylogeny, physiology, and toxigenicity were compared over multiple growth stages. We also examined an isolate from the Gulf of Mexico (Fux et al. 2011) under the same experimental conditions to provide comparison across regions.

Materials and Methods

Isolation and culturing conditions

Four geographical isolates of *Dinophysis* from the United States and Canada were isolated and established in culture (Table 1) following methods described by Tong et al. (2010). The *Mesodinium rubrum* (Lohmann) culture was maintained by feeding it a suspension of *Geminigera cryophila* (Taylor et Lee) prey at the ratio of 1:10 at 4°C in dim light (~50 μmol photons · m^{-2} · s^{-1}) under a 14:10 light:dark photocycle. All cultures were maintained in modified f/2-Si medium (Anderson et al. 1994). After complete consumption of the cryptophyte cells by *M. rubrum*, the ciliate was maintained at 6°C and under 65 μmol photons · m^{-2} · s^{-1} (the experimental conditions) for two days to allow for equilibration, and then provided as prey for *Dinophysis*.

For each *Dinophysis* isolate, triplicate, 2-L Fernbach flasks with 1,300 mL of modified f/2-Si medium were inoculated with ca. 2,000 and 100 cells · mL^{-1} · of experimentally equilibrated *M. rubrum* and *Dinophysis* (inoculated from plateau phase), respectively. Subsamples were removed directly from the flasks three times per week, fixed with a 0.2% v/v Acid Lugol's (Tong et al. 2010), and enumerated for *Dinophysis* and *M. rubrum* cell concentrations using a Sedgewick-Rafter chamber and microscope at 100× magnification.

Light and scanning electron microscopy (LM and SEM)

All cultured *Dinophysis* cells were inoculated, fed and maintained under the conditions described above and then collected during plateau growth phase for morphometric measurement. Preserved (5% v/v formalin) samples were settled in 4°C in the dark for over 24 h. Photographs and cell measurements of *Dinophysis* cells were taken at 400× magnification using a Zeiss Axio Imager A1 microscope equipped with epifluorescence coupled to a Zeiss Axiocam MRc digital camera. Parameters of body length (L), body depth (D), cell area (A), rectangular area of the cell (RA), length of left sulcal list (LSL), anterior cingular list width at the bottom (ACLB), posterior cingular list width at the bottom (PCLB), and ratios of D/L, ACLB/PCLB, LSL/L and A/RA were measured/calculated using the software of Carl Zeiss AxioVision Rel. 4.8 (see demonstration, Fig. 1).

Additionally, *Dinophysis* cells in exponential growth were collected and preserved in 5% with 10% acetate-buffered formalin for SEM. Samples were then dehydrated through a series of alcohol washes into 100% ethyl alcohol and transitioned to 100%

hexamethyldisilazane (HMDS). Built filter assemblies holding 13 mm, 5-μm pore GE PCTE (polycarbonate) membrane filters were used to concentrate the samples. Drying was done at room temperature over 8 h. After drying, the filters were affixed to a SEM stub and coated with gold using an EMS 76 sputter coater. Specimens were observed in a Hitachi S 3400N SEM at St. Petersburg, FL.

DNA extraction, amplification and sequencing

Molecular identification of cultures examined using LM and SEM was performed by DNA sequencing. DNA was extracted from 200 μL of dense culture in exponential growth phase using the Generation Capture Column Kit (Qiagen, Valencia, CA, USA), following the manufacturer's instructions, with a final elution volume of 200 μL. Amplifications were performed in an Eppendorf Mastercycler Nexus thermal cycler (Eppendorf, Hamburg, Germany) with the primers Dinocox1R and Dinocox1F (Lin et al. 2002), which amplify a portion of the mitochondrial cytochrome c oxidase subunit 1 (*cox1*) gene. Polymerase chain reactions (PCRs) contained 1 μl of DNA template (~5 ng), $1 \times$ PCR Buffer (500 mM KCl and 100 mM Tris–HCl, pH 8.3), 2 mM $MgCl_2$, 0.8 mM dNTPs, 0.5 μM of each primer, 0.25 U of AmpliTaq DNA Polymerase (Applied Biosystems Inc., Foster City, CA, USA) and 14.5 μL sterile deionized water for a final volume of 25 μL.

Hot start PCR amplifications included denaturation at 94°C for 10 min, followed by 40 cycles at 94°C for 30 s, 55°C for 1 min, and 72°C for 2 min, and a final extension of 72°C for 10 min. PCR amplification products were visualized by electrophoresis on 1% TAE agarose gel adjacent to a 100 bp DNA ladder. Positive PCR products were cloned into the pGEM®-T Easy vector (Promega Corp., Madison, WI, USA) and clones were screened for inserts by PCR amplification with plasmid primers M13F and M13R. Eight positive clones from each PCR amplicon were selected for DNA sequencing (Eurofins MWG Operon, Ebersberg, Germany). Products were sequenced in both the forward and reverse direction.

DNA sequencing of the DAPA01 clones recovered only pseudogene sequences (See Results, DNA Sequencing for further details); therefore, "reconditioning PCR" experiments were also performed to increase the diversity of sequences obtained from the DAPA01 isolate in an attempt to recover the true *cox1* gene sequence. PCR amplification was performed as described earlier, but the reaction was stopped after 25 cycles. This amplification reaction (6.5 μL) was used as a template in a fresh reaction mixture and cycled 10 more times using the same cycling conditions. The PCR products from this reaction were then cloned and sequenced as described above.

DNA sequence analysis

DNA sequences were manually edited and assembled using Geneious Pro 6.1.2 (Biomatters, Auckland, NZ), and the consensus sequences were compared with those deposited in GenBank using BLAST sequence similarity searches (National Center for Biotechnology Information). To determine the phylogenetic affinities of the *Dinophysis* isolates from the northwestern Atlantic (DAEP01, DAMV01, DABOF02), *cox1* sequences from closely related taxa were downloaded from GenBank and aligned with the sequences generated by this study (Table S1 in the Supporting Information). Attempts to recover the true *cox1* gene

sequence from isolate DAPA01 were unsuccessful; therefore, DNA sequences from this isolate were excluded from further analysis. The alignment was constructed using ClustalW (Thompson et al. 1994) and refined using MUSCLE (Edgar 2004) as implemented in Geneious Pro 6.1.2 (Biomatters, Auckland, NZ). This alignment was subsequently inspected and edited by eye. The final alignment comprised a total of 30 sequences and 519 positions.

Modeltest V. 3.7 (Posada and Crandall, 1998) was used to select the appropriate model of nucleotide substitution for phylogenetic analyses, and phylogenetic trees were constructed using maximum likelihood (ML) analysis and Bayesian inference (BI). *Phalacroma rotundatum* (GenBank Acc. No. EU927470) was used as an outgroup in both analyses. ML analysis was carried out using PhyML (Guindon et al. 2010), with the Tamura Nei (TrN+I) substitution model and 1000 bootstrap replications. Bayesian inference was performed using MrBayes 3.1.2 (Huelsenbeck and Ronquist 2001, Ronquist and Huelsenbeck 2003), with the general time-reversible (GTR) model. Posterior probabilities were estimated using a total of 1,500,000 Markov chain Monte Carlo generations with four parallel chains (one cold and three heated). Trees were sampled every 400 generations following a burn-in period of 500,000 generations. Bayesian posterior probabilities (BPP) were calculated for each clade.

Sample harvesting and extraction of toxins

The three northwestern Atlantic isolates, DAEP01, DAMV01 and DABOF02, were sampled for toxin analysis at three time points during batch-culture growth, from early exponential phase into plateau phase. Triplicate toxin samples were collected at each time point for DAEP01 and DAMV01, however, one triplicate flask of DABOF02 was lost, lending only duplicate samples for each time point. DAPA01, isolated from the Gulf of Mexico, did not increase culture biomass during the experimental period, and therefore, we (1) only harvested cells for toxin analysis at the end-point and (2) pooled triplicates to reach the biomass needed to exceed detection limits for the LC-MS/MS method.

Dinophysis cells were carefully separated from culture medium and both fractions were individually processed and analyzed for OA, DTX1, and PTX2 using instrumentation and methods described previously (Smith et al. 2012). At each sampling point, cells (~180,000) were separated from medium using a 15-μm Nitex sieve. Care was taken during collection to minimize cell damage; cells and mesh were submerged in a Petri dish containing medium to keep the cells wet, and gravity rather than vacuum filtration was utilized. Cells were back washed with fresh f/2-Si medium into a pre-weighed 15-mL centrifuge tube. To determine the actual number of cells harvested (Tong et al. 2010), tubes were gently inverted to homogenize the sample and 200-μL aliquots were transferred to micro-centrifuge tubes containing 1.3 mL of filtered seawater and 3 μl acid Lugol's solution (0.2% v/v) and were enumerated using a Sedgewick-Rafter chamber and microscope at 100× magnification. The 15-mL tube was reweighed to determine the volume of harvested *Dinophysis* cells (sample weight divided by the density of seawater, 1.03 g · mL^{-1}).

Cell concentrates were frozen, thawed, and stored in the dark at room temperature overnight to promote enzymatic hydrolysis of diolester derivatives to parent compounds (Quilliam et al. 1996). Cell lysing was further facilitated using bath sonication (Fisher ultrasonic cleaner, Model FS30H) for 15 min. Extract was subjected to solid phase extraction (SPE) following

Fux et al. (2011). SPE cartridges (Oasis HLB 60 mg; Waters, Milford, MA) were conditioned with methanol (3 mL) and Milli-Q water (3 mL) before being loaded with either harvested cells or medium. SPE cartridges were washed with Milli-Q water (6 mL) and eluted with methanol (1 mL) into 1.5-mL high recovery vials at a flow rate of ~1 mL · min^{-1}. Eluates from the cell and medium samples were heated at 40°C in a heating block, dried under a stream of N_2, and re-suspended in 1 mL of methanol for LC-MS/MS toxin analysis.

Toxin analysis

Analysis was performed on a liquid-chromatography tandem mass spectrometry (LC-MS/MS) system, which consisted of an Agilent 1100 HPLC coupled to a Quattro Micro triple quadrupole (TQ) mass spectrometer (Waters Micromass) as described by Smith et al. (2012). Separation was achieved on a C8 Hypersil column (50 × 2.1 mm; 3.5 μm particle size) maintained at 25°C. The flow rate was set at 0.25 mL · min^{-1} and a volume of 10 μL was injected. Binary mobile phase was used, with phase A (100% aqueous) and phase B (95% aqueous acetonitrile (ACN), both containing 2 mM ammonium formate and 50 mM formic acid. A gradient elution was employed, starting with 30% B, increased to 100% B over 9 min, held for 3 min, then decreased to 30% B in 0.1 min and held for 3 min to equilibrate at initial conditions before the next run started. The TQ was operated in multiple reaction monitoring (MRM) mode and the following transitions were monitored in the same run: OA, m/z 803.5>255.5 and 803.5>803.5; DTX1, m/z 817.5>255.5 and 817.5>817.5 in negative ionization mode and PTX2, m/z 876.5>213.0 in positive ionization mode. OA and DTX1, or PTX2 were quantified against 7 level calibration curves obtained with OA or PTX2 reference solutions (NRC-Canada), respectively.

Toxin data are presented as cellular toxin content or quota (toxin amount per cell), extracellular toxin concentration (toxin amount dissolved in a mL of culture medium) and the percentage of toxins contained in the cellular vs. extracellular compartments (e.g., cellular toxin amount per mL / cellular + extracellular toxin · mL^{-1} * 100%). In the latter calculation only, the initial amount of dissolved toxin transferred from the inoculant cultures into the experimental flasks was subtracted from the extracellular toxin raw values before calculating the percent partitioning between the two culture compartments over growth. DTX1 toxin content data for DAEP01 and DAMV01 were log transformed to reach normality before statistical analyses were performed; all other data sets were normally distributed. Mixed Model, Repeated Measures ANOVA (SAS software, version 9.2) was used to analyze for 1) differences in cellular DSP toxin content *between* isolates and 2) differences in absolute toxin quotas and concentrations *within* isolates over the cultures' growth cycle. Alpha was set at 0.05 for all analyses.

Results

Microscopy

Three isolates from coastal waters of the northwestern Atlantic (DAEP01, DAMV01 and DABOF02), previously identified as *D. acuminata* (Fux et al. 2011), and one isolate from the Gulf of Mexico (DAPA01) were studied using light and electron microscopy (Figs. 2 and 3).

All isolates were collected at the beginning of stationary phase for LM and at exponential growth phase for SEM.

Dinophysis acuminata morphotypes DAEP01, DAMV01 and DABOF02 possessed the typical morphology of their genus in that they had a distinctive funnel-shaped anterior cingular list and were differentiated from other species by their size and body shape. Cells were almost oval or elliptical. The posterior profile was rounded while the left sulcal list was well developed, supported by three ribs and extending to just over halfway down the ventral margin of the hypotheca. In more detail, the main hypothecal plates were generally weakly convex in the lateral and ventral views of *D. acuminata*. The plates were almost straight-sided, or with a straight dorsal edge (Figs. 2 a, b and c; 3). The hypotheca was rounded and either smooth or with one to four knob-like protuberances of irregular size (Fig. 2a). SEM analysis showed that the cell theca was areolate, with each areola having a pore (Fig. 3a). A megacytic zone (Fig. 3f) was located at the dorsal –ventral side of the well fed *Dinophysis* isolate, DABOF02. No areolae pores were observed in the megacytic zone. Cells were differentiated by size not only between isolates, but also within clonal cultures (Fig. 3e and Table 2). Larger and smaller cells occurred in the same SEM picture, DABOF02, with the depth of 31.11 and 24.43 μm, respectively. SEM revealed thecal ultrastructure typical of the *D. acuminata* complex: membranous cingular and sulcal lists, thecal surface markings, megacytic area, and the large hypothecal plates. The peduncular capture of prey, *M. rubrum*, by *Dinophysis* was also observed and imaged by SEM (Fig. 4, a and b).

Cell size measurements were made on the four *Dinophysis* isolates to determine if they could be differentiated morphometrically. *D. acuminata* DAEP01, Figure 2a, was the smallest isolate of all four strains, having the shortest cell length, depth, anterior cingular list at the bottom, posterior cingular list at the bottom, and left sulcal list, and the smallest area and rectangular area (Table 2 and Fig. 2a). In lateral view, DAEP01 was elongated and narrow to oval with or without ventrally placed antapical protuberances (Figs. 2a; 3a and b). *D. acuminata* DAMV01 and DABOF02, Figures 2, b and c, were the more moderate-sized cells, compared with the other isolates. DAMV01 had significantly longer ACLB and depth, but shorter LSL than DABOF02. Antapical protuberances were also found in DAMV01 cells, but not in DABOF02. The DAPA01 isolate, from the Gulf of Mexico, was in the *D. acuminata* complex but more closely resembles *D.* cf. *ovum* (Fux et al. 2011). This isolate differed from the three *D. acuminata* isolates morphologically (One-way ANOVA, Table 2; Figs. 2d and 5).

Three similar *D. acuminata* morphotypes, DAEP01, DAMV01 and DABOF02, and *D.* cf. *ovum*, DAPA01, were all differentiated based on morphometrics under light microscopy. The Martha's Vineyard isolate was most similar to the Bay of Fundy isolate while clearly the Texas isolate was morphologically different and larger than all others (Fig. 5; Table 2). The Variable Area metric produced the same results as Rectangular Area, and therefore, both were not necessary for classification purposes. Eel Pond had the smallest cells, while the Bay of Fundy was the least variable isolate, morphometrically. Of the morphometric traits used for the four isolates, the length of the body was the most conservative, and the depth of the body and the length of the left sulcal list were the most variable. Morphologically, the three North American isolates conform to the species description of *D. acuminata*.

DNA sequencing

DNA sequencing successfully recovered the expected mt *cox1* gene sequence for all but the DAPA01 isolate from the Gulf of Mexico. Sequences of DAEP01, DAMV01 and DABOF02 (GenBank Accession No. KJ670071, KJ670072 and KJ670073, respectively) ranged from 957–1007 bp, and were 100% identical to each other over the aligned region. Clones of the *cox1* pseudogene DAPA01were 909–935 bp in length, and each contained a 198-bp long sequence that was unrelated to the *cox1* gene (GenBank Accession No. KJ670074). This insert was located at nucleotide positions 478–746 (compared with *Durinskia baltica*, GenBank Acc. No. JX001479, as in Raho et al. 2013), which is similar to the location of the pseudogene insert recovered by Raho et al. (2013) from *Dinophysis saccula* (GenBank Acc. No. KC592387). BLAST sequence similarity searches comparing the pseudogene insert with sequences deposited in GenBank indicated that the insert showed no homology to any sequences in this database. A separate sequence comparison following removal of the pseudogene region showed that DAPA01 was distinguished from DAEP01, DAMV01, and DABOF02 by a single bp difference. Despite multiple cloning and sequencing attempts, we were unable to recover the full length sequence of the true gene and reconditioning experiments were similarly unsuccessful; therefore, this isolate was excluded from the phylogenetic analyses.

Phylogenetic analysis

Tree topologies generated using ML and BI were identical, and the phylogenetic relationships among the species were similar to those reported previously (Papaefthimiou et al., 2010; Raho et al., 2013). These analyses recovered three well-supported main clades (Fig 6): the first comprised *D. acuta* and *D. norvegica*, the second comprised *D. tripos* and *D. caudata*, and the third comprised the "*acuminata* complex", which included *D. acuminata, D. ovum, D. saccula*, and *D. skagi* (the "small cell" growth form of *D. saccula* and *D. acuminata*; see Reguera and Gonzalez-Gil, 2001). Within the *tripos + caudata* clade, the *D. tripos* isolate from Spain (JF803843) grouped with the *D. caudata* isolate (HQ681269), also from Spain, while the remaining isolates in this group originated from the northern and northwestern Atlantic. The *cox1* sequences obtained from DAMV01, DABOF02, and DAEP01 grouped with taxa comprising the "*acuminata*" complex and were identical or nearly identical to *D. acuminata* from the northwestern Atlantic, *D. ovum* from Spain and Greece, and one strain of *D. saccula* from Spain. Within the *acuminata* complex, sequences of *D. acuminata* (AM931582) and *D. skagi* (HQ681273), both from Spain, clustered in a well-supported clade.

Growth and toxin

Three isolates of *Dinophysis* spp. from northwestern Atlantic waters (DAMV01, DABOF02, and DAEP01) were cultured concurrently under the same conditions, and their growth rates and toxigenicity compared across growth stages. When possible, the three northern isolates were also compared to a geographically-distinct isolate from the Gulf of Mexico (DAPA01), grown under the same laboratory conditions and at the same time. Physiological experiments on DAPA01 failed, likely due to this isolate's reduced tolerance for the low inoculation temperatures required for the prey species, 6°C; this isolate's lack of growth under

experimental conditions, and subsequent expiration, limited the present study to an end-point toxin measurement and toxin profile. As such, the outlier was excluded from all growth and toxigenicity figures but is described in the text for comparison.

Two subgroups were observed amongst the three northwestern Atlantic *Dinophysis* isolates based on: 1) elevated growth rate, greater biomass at stationary phase, production of and DAEP01); and 2) reduced growth rate and biomass, production of only DTX1 and PTX2, and no detectable growth-induced change in toxin content (DABOF02). DAPA01 from the Gulf of Mexico, however, did not grow well under these experimental conditions, contained only OA, and the maximum cellular OA content, 12.56 pg · cell^{-1} was ca.10 times greater than total DSP toxin levels measured in the three northern isolates.

All three of the northwestern Atlantic *Dinophysis* isolates were inoculated in plateau phase with the same isolate of *M. rubrum* as the prey species. After a 3 d lag, the three northwestern Atlantic isolates followed a characteristic pattern of growth, with exponential and plateau phases (Fig. 7). Moreover, the isolate DABOF02 had a longer exponential growth, 23 d, compared to DAEP01 and DAMV01, both of which had 13 d of exponential growth. Geographical variations were also found in their growth rate. DAEP01 and DAMV01 had similar growth rates of 0.20 ± 0.01 and 0.20 ± 0.02 d^{-1}, respectively (Fig. 7), whereas DABOF02 from the Bay of Fundy had a significantly lower growth rate (0.15 ± 0.05 d^{-1}; Kruskal-Wallis test, $p<0.05$). This reduction in growth may be a consequence of a slower feeding rate by DABOF02 as the ciliate prey was entirely consumed by the 11th and 13th d in DAEP01 and DAMV01 cultures, but remained in culture another 10 d when incubated with the DABOF02 isolate (Fig. 7).

The toxin profiles for the three northwestern Atlantic isolates were compared over the cultures' growth. DAEP01 and DAMV01 had similar toxin profiles, producing PTX2, OA and DTX1. DABOF02, from the Bay of Fundy, however, produced only PTX2 and DTX1 at detectable levels. A large amount of biomass (>2,000,000 cells) of DABOF02 was then extracted for toxin analysis and confirmed the absence of OA. The cellular OA content in DAEP01, 0.38 to 0.90 pg · cell^{-1}, was significantly greater than levels measured in DAMV01, 0.12 to 0.32 pg · cell^{-1}. In contrast, cells of DAMV01 contained significantly more DTX1 (1.1 to 1.8 pg · cell^{-1}) when compared to DAEP01 (0.35 to 0.65 pg · cell^{-1}) and DABOF02 (0.26 to 0.34 pg · cell^{-1}). PTX2 was the dominant cellular component of the three isolates, ranging from 8.2 to 15.1 in DAEP01, 8.7 to 17.3 in DAMV01, and 13.0 to 21.8 pg · cell^{-1} · in DABOF02. As such, PTX2 comprised 92±2%, 88±1%, and 98±1% of the cellular toxin profile in each isolate, respectively.

Cellular toxin quotas of okadaic acid, DTX1, and PTX2 in DAEP01 and DAMV01 followed a similar pattern: beginning low during exponential growth, increasing by early to middle plateau phase, and decreasing by late plateau phase to return to initial toxin quotas (Fig. 8, a–c). The isolate from the Bay of Fundy, Canada (DABOF02) was again distinct from the other two northwestern Atlantic isolates, with cellular DTX1 remaining constant over growth, and PTX2 only changing at the end of the growth cycle, showing a significant decrease at plateau phase.

Extracellular toxins, or dissolved toxin in the culture medium, again demonstrated differences between DABOF02 and the other two northwestern Atlantic isolates. The concentration of extracellular OA, DTX1, and PTX2 remained low and constant over growth in the DABOF02 isolate (Fig. 8, d–f). In contrast, the medium in DAMV01 contained significantly more extracellular DTX1 and PTX2 by early plateau phase, and DAEP01 contained significantly more extracellular DTX1 by late plateau phase and PTX2 by early plateau phase.

The three northwestern Atlantic *Dinophysis* isolates were further investigated for toxin partitioning between cellular and extracellular components during batch culture growth (Fig. 9). The same toxins were detected both in the cells and in the medium during exponential, early and late plateau phases. Over the growth phases sampled, the cells of DAEP01 and DAMV01 contained 49–68% and 41–68%, respectively, of the total OA present in the culture (Fig. 9a). Relatively less DTX1 was contained in the cells, as only 38–52%, 23–34% and 36–100% of the total was intracellular in DAEP01, DAMV01 and DABOF02, respectively (Fig. 9b). While the majority of DTX1 in the culture appeared to be extracellular, the majority of PTX2 was associated with the cellular fraction over all three growth phases, with cellular PTXs comprising 81–91% of the total PTX2 within the DAEP01 culture, 84–93% in DAMV01, and 89–91% in DABOP02 (Fig. 9c).

Discussion

Morphological and phylogenetic analyses

Isolates were classified as being of the *Dinophysis "acuminata"* complex, and more specifically as *D. acuminata* or *D.* cf *ovum*, through a combination of morphological and molecular analyses. Morphologically, all of the isolates from the northwestern Atlantic (DAEP01, DAMV01 and DABOF02) conformed to the species description of *D. acuminata*: cell with rounded hypotheca and a left sulcal list supported by three ribs; rounded symmetrically when viewed laterally; cells much longer than broad; and hypotheca rounded, with or without antapical protruberances (Dodge 1982). Molecular analyses grouped the three northwestern Atlantic isolates with taxa comprising the "*acuminata*" complex based on *cox1* sequences. Isolates were identical or nearly identical to other *D. acuminata* from the northwestern Atlantic, *D. ovum* from Spain and Greece, and one strain of *D. saccula* from Spain. The larger-bodied isolate from the Gulf of Mexico, DAPA01 (Table 2) also keyed out as belonging in the "*acuminata*" complex; however, this outlier was morphologically more related to *D.* cf. *ovum.* Phylogenetic analysis of DAPA01 was impossible despite numerous attempts due to the presence of a pseudogene, which contained a 198-bp long insert unrelated to any sequence in the GenBank database. Interestingly, Raho et al. (2013) previously reported two pseudogene inserts in the *cox1* gene of *D.saccula*, both of which were located similarly to the insert we observed; however, unlike this study, we were unable to recover the true *cox1* gene along with the pseudogene.

There was a combination of morphological characteristics that made each *D. acuminata* isolate recognizable from its conspecifics (e.g., DAEP01 had a narrower anterior cingular list width at the bottom (ACLB), posterior cingular list width at the bottom (PCLB), length of the body (L), depth of the body (D) and length of the sulcal list (LSL), Fig. 5), suggesting

subpopulations existed in the region and could possibly be identified in field material using a specific set of characteristics. In populations of *Alexandrium fundyense* from the Gulf of Maine region, temporal and spatial genetic differentiation were detected using microsatellite markers (Erdner et al. 2011, Richlen et al. 2012). Rynearson et al. (2006) also used microsatellite markers to identify two genetically distinct populations of the diatom *Ditylum brightwellii* within a single location. These authors speculated that environmental selection influenced bloom dynamics of this species. This certainly could apply to dinoflagellates as well at ecologically significant time scales (Shankle et al. 2004) and should be an objective of future investigations into *Dinophysis* population dynamics and structure.

In addition to population genetics and environmental selection, life cycle stages also contribute to species polymorphism (Reguera et al. 2012). The identification of a cell as *Dinophysis acuminata* is sometimes *D.* cf. *acuminata* meaning "most similar to." Classic taxonomy and identification of *Dinophysis* follow Kofoid and Skogsberg (1928), and from that beginning, identification has progressed to the stage where the following characters are used to separate the species (accepting *Phalacroma* as a separate genus): dorsal and ventral cell curvature, relative length and shape of the left and right sulcal lists, positioning of the three ribs that support the left sulcal list, ventral view, and dorsal-ventral depth of the epitheca (Steidinger and Tangen 1997). However, it sometimes can be difficult to identify an individual specimen with certainty because of morphological plasticity and cell orientation.

Despite species designation, there was variability within each clonal culture (Fig. 5), further highlighting the plasticity of this species. A few cells of each clone more closely resembled *D. ovum*, demonstrating overlap within the *D. "acuminata"* complex. Polymorphism also exists across regions as our results (Table 2) are in direct contrast to Raho et al. (2008) who concluded that cells of *D. acuminata* were larger than *D. ovum* (both from Spain). In addition, the cell sizes of the three *D. acuminata* isolates examined here (Table 2) were within the lower range of *D. acuminata* from Spain: length of 40–59 μm and width of 24–43 μm (Hargraves and Maranda 2002, Raho et al. 2008). The cell sizes of *D.* cf *ovum* from the Gulf of Mexico (DAPA01), in contrast, were larger than the *D. ovum* characterized from Spain, with the latter only measuring 32–42 μm in length and 22.5–32 μm in depth.

The Dinophysiales typically have <20 thecal plates arranged in recurring series such as epithecal and hypothecal,, but unlike the Gonyaulacales and Peridiniales, the order hasn't undergone scrutiny at different levels of resolution to differentiate pseudocryptic species, as has been done for *Heterocapsa* (Iwataki, 2008) and *Gambierdiscus* (Litaker et al. 2010). In addition to recognition of pseudocryptic species, there can be subpopulation differences that can be designated as "strains". This is essentially another level of biodiversity and how it should be treated in management of toxic algal blooms and phytoplankton ecology has not been clarified. At what level of adaptation/evolution is it important to distinguish between identifiable biounits, or is the level of resolution dependent on the specific purpose of the investigation? Lakeman et al., (2009) provide a discussion of the strain concept in phytoplankton as well as a discussion of selection processes and "in-culture evolution".

Physiology and toxigenicity

Isolates from the northwestern Atlantic were classified as being of the *Dinophysis "acuminata"* complex, and more specifically as *D. acuminata* (DAEP01, DAMV01, DABOF02), through examination of their mixotrophic growth, patterns of toxin accumulation and extracellular release, and toxin profiles. Upon the inoculation of *Mesodinium rubrum* into *D. acuminata* cultures, the dinoflagellates rapidly consumed the ciliate prey. Within days of the prey being depleted from the culture, dinoflagellates transitioned to early plateau phase and accumulated maximum levels of DSP and PTX toxins in cells (Fig. 8). Once *Dinophysis* cells reached late plateau phase, maximum densities were achieved, the amount of toxin contained in the cells decreased, and the medium reached maximum concentrations of total DSP toxins and PTX2, suggesting accelerated toxin exudation as a result of cell aging or death. Interestingly, we also detected significant increases in some extracellular toxins as soon as early plateau phase, providing evidence for active toxin exudation during periods of growth. The isolate from the Bay of Fundy, DABOF02, displayed less growth-dependent variation in toxin production or extracellular release. The toxin profiles, including OA and/or DTX1 and PTX2, of the three northwestern Atlantic isolates are consistent with previous reports for other *D. acuminata* isolates (Table 3) and field material, including a recent bloom consisting of mostly *D. acuminata* off the coast of Washington State (Trainer et al. 2013). Seven isolates of *D. acuminata* from Denmark, however, produced only PTX2 and no DSP toxins (Nielsen et al. 2012).

The simpler toxin profile of the isolate from the Gulf of Mexico (DAPA01) consisted of only okadaic acid, classifying the outlier as being more similar to *D.* cf. *ovum* (Raho et al. 2008, Campbell et al. 2009, Deeds et al. 2010) than *D. acuminata*. Species classifications support those made with SEM images and morphological measurements. Interestingly, the *D.* cf. *ovum* isolate was also different from the three *D. acuminata* isolates in that it did not follow the typical mixotrophic growth cycle; DAPA01 was unable to increase its biomass under the same culturing conditions, and instead only divided enough to maintain survival. The lack of culture growth indicates a reduced temperature tolerance or different prey preference for this warmer-climate isolate that might impede invasion into more temperate water masses.

The three northwestern Atlantic *Dinophysis* isolates were further investigated for the extracellular release of toxins and partitioning between intracellular and extracellular components during batch culture growth (Fig. 9). Although we detected a significant release of PTX2 into the medium during growth, the majority of total PTX2 was retained within the cells or associated with cell debris. Together this suggests that PTX2 is preferably retained within the cell and/or has a strong affinity for cellular debris upon exudation, a concept originally proposed using field material (MacKenzie et al., 2004). This finding was in agreement with previous studies that reported 94.9% of the total PTX2 was found within well-fed *D. acuminata* cells, 98.2% in *D. fortii* cells (Nagai et al. 2011), 73–78% in *D. acuminata* cells exposed to prolonged starvation (Smith et al. 2012) and over 50% in *D. acuta* cells (Nielsen et al. 2013). In contrast to PTX2, the majority of total DTX1 was dissolved in the medium, i.e., released from cells, over the growth cycle. Furthermore, we observed significant increases in extracellular DTX1 as early as early plateau phase. Nagai

et al. (2011) similarly reported a remarkable increase in the concentration of extracellular toxins during exponential and early-mid plateau growth, concluding that *Dinophysis* cells were actively exuding toxin during periods when cells were not dying.

Although the three *D. acuminata* isolates were more similar to each other than to *D.* cf. *ovum* from the Gulf of Mexico, variability was observed between conspecifics (Figs. 8 and 9), suggesting the existence of subpopulations and supporting the addition of a spatially explicit extension, e.g., *D. acuminata* Eel Pond, *D. acuminata* Martha's Vineyard, *D. acuminata* Bay of Fundy, etc. (Steidinger, 2009). Isolates from Eel Pond (DAEP01) and Martha's Vineyard, (DAMV01) had similar growth rates, produced OA, DTX1 and PTX2, and contained maximum toxin levels during early plateau phase; however, differences in the toxin profiles existed. The Eel Pond isolate contained similar amounts of cellular OA and DTX1, while DAMV01 contained significantly more DTX1 than OA. Once all DSP derivatives were summed, however, the overall toxin quotas were similar between these two isolates, with DAMV01 possessing only slightly more maximum total DSP toxin, 2.1 pg · $cell^{-1}$, than DAEP01, 1.6 pg · $cell^{-1}$ (Table 3). *Dinophysis acuminata* from the Bay of Fundy, Canada (DABOF02) had a significantly reduced growth rate and biomass when compared to the other two isolates of this species, produced only DTX1 and PTX2, and contained an order of magnitude less DSP toxin per cell (maximum of 0.3 pg DTX1 · $cell^{-1}$, Table 3), making differentiation of this conspecific possible in field material if the subpopulation was isolated in time or space. Together this suggests sub-regional variability in the potential toxicity within the northwestern Atlantic, such that the Vineyard Sound　Eel Pond, MA > Bay of Fundy.

Dinophysis acuminata from the northwestern Atlantic generally contained less cellular DSP toxin in batch culture than isolates and field material from other regions (Table 3), including *D.* cf. *ovum* (DAPA01) that contained 10× more okadaic acid. The three *D. acuminata* isolates contained 0.01 – 1.8 pg · $cell^{-1}$ of OA or DTX1 in batch culture, a value less than or at the lower end of *D. acuminata* isolates from Japan, 0.2 – 12.2 pg · $cell^{-1}$ (Kamiyama and Suzuki 2009, Kamiyama et al. 2010, Nagai et al. 2011) and Brazil, 3.2 – 18.0 pg · $cell^{-1}$ (Mafra et al. 2013). Currently, there are no other isolates of the *D. "acuminata"* complex maintained in culture to provide a comparison. In natural populations, maximum cell quotas can be one to two orders of magnitude higher than these culture levels, such as the reported maximum cell quotas of 158 pg OA · $cell^{-1}$ along the coast of France in May (Marcaillou et al. 2005) and 72 pg OA · $cell^{-1}$ in field material from Denmark (Jørgensen and Andersen, 2007). Similarly, *D. acuminata* in field material off the U.S. west coast contained more OA equivalents (OA+DTX1+DTX3) per cell, ranging from 1.14 to 8.80 pg · $cell^{-1}$ (calculated from Table 1 in Trainer et al. 2013), than our conspecifics isolated from the east coast of the U.S. and Canada. These elevated toxin quotas off the coast of Washington State, which were associated with contaminated shellfish and harvest closures, are instead more similar to quotas (DAPA01, 12.56 pg OA · $cell^{-1}$) detected in our *D.* cf. *ovum* isolate that was collected during the 2008 closures in the Gulf of Mexico due to DSP toxin contamination of shellfish (Campbell et al. 2009, Deeds et al. 2010). The relatively low toxin per cell quotas of the northwestern Atlantic isolates is consistent with the very low number of shellfish closures in that region due to DSP toxins – a finding first reported by Hackett et al. (2009) for the Eel Pond isolate, but now relevant to isolates from the Bay of Fundy and Vineyard

Sound as well. Recently, however, Hattenrath-Lehman et al. (2013) reported an alarming concentration of DSP toxins in shellfish (i.e., eight times the regulatory limit) in Northport Bay, NY that was associated with an extensive bloom of minimally toxic *D. acuminata*: 396 $\pm$ 321 fg OA $\cdot$ cell^{-1}; 1, 238 $\pm$ 164 fg DTX1 $\cdot$ cell^{-1}; 1,680 $\pm$ 1,314 fg PTX $\cdot$ cell^{-1}. Therefore, despite the low toxin per cell quotas of our *Dinophysis* isolates, the overall potential for DSP toxicity in the larger region may actually be considered low to moderate and warrants further investigation.

As the toxicity and mode of action of pectenotoxins is not well characterized yet, this group of phycotoxins was excluded from this inference; however, it is important to note that our three northwestern Atlantic *D. acuminata* isolates contained 8.2 to 19.2 pg PTX2 $\cdot$ cell^{-1}, values well within the range of quotas reported by many regions, including coastal waters from Korea, Norway, New Zealand, and Japan, and seven isolates of *D. acuminata* from Denmark (Nielsen et al. 2012; Table 3). Higher toxin quotas have only been reported in a natural population off the coast of Chile that contained 180 pg PTX2 $\cdot$ cell^{-1} and an isolate from Japanese waters that contained 107.5 pg PTX2 $\cdot$ cell^{-1} $\cdot$ (Kamiyama et al. 2010).

Diol-ester derivatives were previously reported at relatively low levels in these isolates (Fux et al. 2011), but were not investigated as part of the current work. In the previous, more explorative study using these isolates, large culture volumes were harvested at a single end point (i.e., 1 million cells collected during plateau phase) and immediately boiled to preserve the original toxin profile. This method provided concentrated samples for the LC-MS/MS that were characterized using parent and daughter scans, and selective reaction monitoring of all possible derivatives that had been previously described in other strains. The current work, instead, had the aim of comparing patterns of growth and toxin production of major toxicants over the growth cycle and characterizing regional differences based on morphological and phylogenetic properties. With the addition of multiple time points to the design, culture biomass needed to be reduced for each toxin sample (180,000 cells). To compensate for these lower levels of toxins per sample, samples were not boiled, and instead, were kept at room temperature overnight after a freeze-thaw to allow for enzymatic hydrolysis of diols to parent compounds (Quilliam et al. 1996). With this modified method, we were able to exceed detection limits of the LC-MS/MS for the major toxins and provide new comparative information with respect to toxin production and extracellular release over the growth cycle.

Conclusions

All three northwestern Atlantic isolates were classified as being *D. acuminata* according to morphological measurements and microscopy, phylogenetic analysis, and toxigenicity; however, there was evidence of phenotypic heterogeneity that supports the addition of a spatially explicit extension, e.g., *D. acuminata* Eel Pond, *D. acuminata* Martha's Vineyard, *D. acuminata* Bay of Fundy (Steidinger 2009). The observed variability in *D. acuminata* is highly suggestive of spatial (and/or temporal) population structure and subspecific resolution may be helpful in characterizing and predicting bloom dynamics, including potential toxicity. This study demonstrated the presence of relatively low-toxicity phenotypes of *D. acuminata* in the northwestern Atlantic, a region with infrequent shellfish harvesting

closures due to DSP toxins. If this pattern is repeated with analyses of more geographically and temporally dispersed isolates from the region, it would appear that the risk of significant DSP toxin outbreaks is low to moderate in this area of the U.S.

Acknowledgments

Abbreviations

ACLB	anterior cingular list width at the bottom
CCMP	Provasoli-Guillard Center for Culture of Marine Phytoplankton
***cox*1**	cytochrome c oxidase I
DTX	dinophysistoxin
DSP	diarrhetic shellfish poisoning
LC-MS	liquid chromatography-mass spectrometry
nd	not detected
OA	okadaic acid
PCLB	posterior cingular list width at the bottom
PTX	pectenotoxin
tr	trace level

References

Anderson DM, Kulis DM, Doucette GJ, Gallager JC, Balech E. Biogeography of toxic dinoflagellates in the genus *Alexandrium* from the northeast United States and Canada as determined by morphology, bioluminescence, toxin composition, and mating compatibility. Mar Biol. 1994; 120:467–478.

Blanco J, Alvarez G, Uribe E. Identification of pectenotoxins in plankton, filter feeders, and isolated cells of a *Dinophysis acuminata* with an atypical toxin profile, from Chile. Toxicon. 2007; 49:710–716. [PubMed: 17189646]

Campbell L, Olson RJ, Sosik HM, Abraham A, Henrichs DW, Hyatt CJ, Buskey EJ. First Harmful *Dinophysis* (Dinophyceae, Dinophysiales) Bloom in the US is revealed by automated imaging flow cytometry. J Phycol. 2010; 46:66–75.

Deeds JR, Wiles K, Heideman GB, White KD, Abraham A. First US report of shellfish harvesting closures due to confirmed okadaic acid in Texas Gulf coast oysters. Toxicon. 2010; 55:1138–1146. [PubMed: 20060850]

Dodge, JD. Marine Dinoflagellates of the British Isles. Her Majesty's Stationery Office; London: 1982.

Edgar RC. MUSCLE: multiple sequence alignment with high accuracy and high throughput. Nucleic Acids Res. 2004; 32:1792–1797. [PubMed: 15034147]

Edvardsen B, Shalchian-Tabrizi K, Jakobsen KS, Medlin LK, Dahl E, Brubak S, Paasche E. Genetic variability and molecular phylogeny of *Dinophysis* species (Dinophyceae) from Norwegian waters inferred from single cell analyses of rDNA. J Phycol. 2003; 39:395–408.

Erdner DL, Richlen M, McCauley LAR, Anderson DM. Diversity and dynamics of a widespread bloom of the toxic dinoflagellate *Alexandrium fundyense*. PloS one. 2011; 6:e22965. [PubMed: 21829565]

FAO. Marine Biotoxins Food and Agriculture Organization of the United Nations, Rome. 2004.

Fux E, Smith JL, Tong MM, Guzman L, Anderson DM. Toxin profiles of five geographical isolates of *Dinophysis* spp. from North and South America. Toxicon. 2011; 57:275–287. [PubMed: 21147146]

Gómez F. A checklist and classification of living dinoflagellates (Dinoflagellata, Alveolata). CICIMAR Océanides. 2012; 27:65–140.

Guindon S, Dufayard JF, Lefort V, Anisimova M, Hordijk W, Gascuel O. New algorithms and methods to estimate maximum-likelihood phylogenies: assessing the performance of PhyML 3.0. System Biol. 2010; 59:307–321. [PubMed: 20525638]

Hackett JD, Tong MM, Kulis DM, Fux E, Hess P, Bire R, Anderson DM. DSP toxin production de novo in cultures of *Dinophysis acuminata* (Dinophyceae) from North America. Harmful Algae. 2009; 8:873–879.

Hargraves PE, Maranda L. Potentially Toxic Or Harmful Microalgae From The Northeast Coast. Northeastern Naturalist. 2002; 9:81–120.

Hattenrath-Lehmann TK, Marcoval MA, Berry DL, Fire S, Wang Z, Morton SL, Gobler CJ. The emergence of *Dinophysis acuminata* blooms and DSP toxins in shellfish in New York waters. Harmful Algae. 2013; 26:33–44.

Huelsenbeck JP, Ronquist F. MRBAYES: Bayesian inference of phylogenetic trees. Bioinformatics. 2001; 17:754–755. [PubMed: 11524383]

Johnson M. The acquisition of phototrophy: adaptive strategies of hosting endosymbionts and organelles. Photosynth Res. 2011; 107:117–132. [PubMed: 20405214]

Jørgensen K, Andersen P. Relation between the concentration of *Dinophysis acuminata* and diarrheic shellfish poisoning toxins in blue mussels (Mytilus edulis) during a toxic episode in the Limfjord (Denmark), 2006. J Shellfish Res. 2007; 26:1081–1087.

Kamiyama T, Nagai S, Suzuki T, Miyamura K. Effect of temperature on production of okadaic acid, dinophysistoxin-1, and pectenotoxin-2 by *Dinophysis acuminata* in culture experiments. Aquat Microb Ecol. 2010; 60:193–202.

Kamiyama T, Suzuki T. Production of dinophysistoxin-1 and pectenotoxin-2 by a culture of *Dinophysis acuminata* (Dinophyceae). Harmful Algae. 2009; 8:312–317.

Kifle D, Purdie DA. The seasonal abundance of the phototrophic ciliate *Mesodinium rubrum* in Southampton Water, England. J Plankton Res. 1993; 15:823–833.

Kim JH, Lee KJ, Suzuki T, Kang YS, Kim PH, Song KC, Lee TS. Seasonal Variability of Lipophilic Shellfish Toxins in Bivalves and Waters, and Abundance of *Dinophysis* spp. In Jinhae Bay, Korea. J Shellfish Res. 2010; 29:1061–1067.

Kofoid, CA., Skogsberg, T. Commander L.M. Garrett, U.S.N., Commanding. [No.] XXXV. The Dinoflagellata: the Dinophysoidae., Memoirs of the Museum of Comparative Zoölogy. Harvard College; Cambridge, Massachusets: 1928. Reports on the scientific results of the expedition to the Eastern Tropical Pacific, in charge of Alexander Agassiz, by the U.S. Fish Commission Steamer "Albatross" from October 1904 to March 1905 Lieut; p. 1-766.

Lakeman MB, von Dassow P, Cattolico RA. The strain concept in phytoplankton ecology. Harmful Algae. 2009; 8:746–758.

Lin S, Zhang H, Spencer DF, Norman JE, Gray MW. Widespread and Extensive Editing of Mitochondrial mRNAS in Dinoflagellates. J Mol Biol. 2002; 320:727–739. [PubMed: 12095251]

MacKenzie L, Beuzenberg V, Holland P, McNabb P, Selwood A. Solid phase adsorption toxin tracking (SPATT): a new monitoring tool that simulates the biotoxin contamination of filter feeding bivalves. Toxicon. 2004; 44:901–918. [PubMed: 15530973]

MacKenzie L, Beuzenberg V, Holland P, McNabb P, Suzuki T, Selwood A. Pectenotoxin and okadaic acid-based toxin profiles in *Dinophysis acuta* and *Dinophysis acuminata* from New Zealand. Harmful Algae. 2005; 4:75–85.

Mafra LL Jr, Tavares CPdS, Schramm MA. Diarrheic toxins in field-sampled and cultivated *Dinophysis* spp. cells from southern Brazil. J Appl Phycol. 2013

Marcaillou C, Mondeguer F, Gentien P. Contribution to toxicity assessment of *Dinophysis acuminata* (Dinophyceae). J Appl Phycol. 2005; 17:155–160.

Marin I, Aguilera A, Reguera B, Abad JP. Preparation of DNA suitable for PCR amplification from fresh or fixed single dinoflagellate cells. Biotechniques. 2001; 30:88-. [PubMed: 11196325]

Miles CO, Wilkins AL, Munday R, Dines MH, Hawkes AD, Briggs LR, Sandvik M, Jensen DJ, Cooney JM, Holland PT, Quilliam MA, MacKenzie AL, Beuzenberg V, Towers NR. Isolation of pectenotoxin-2 from *Dinophysis acuta* and its conversion to pectenotoxin-2 seco acid, and preliminary assessment of their acute toxicities. Toxicon. 2004a; 43:1–9. [PubMed: 15037023]

Miles CO, Wilkins AL, Samdal IA, Sandvik M, Petersen D, Quilliam MA, Naustvoll LJ, Rundberget T, Torgersen T, Hovgaard P, Jensen DJ, Cooney JM. A novel pectenotoxin, PTX-12, in *Dinophysis* spp and shellfish from Norway. Chem Res Toxicol. 2004b; 17:1423–1433. [PubMed: 15540940]

Nagai S, Suzuki T, Nishikawa T, Kamiyama T. Differences in the Production and Excretion Kinetics of Okadaic Acid, Dinophysistoxin-1, and Pectenotoxin-2 between Cultures of Dinophysis Acuminata and Dinophysis Fortii Isolated from Western Japan. J Phycol. 2011; 47:1326–1337. [PubMed: 27020356]

Nielsen L, Krock B, Hansen P. Effects of light and food availability on toxin production, growth and photosynthesis in *Dinophysis acuminata*. Mar Ecol Prog Ser. 2012; 471:37–50.

Nielsen LT, Krock B, Hansen PJ. Production and excretion of okadaic acid, pectenotoxin-2 and a novel dinophysistoxin from the DSP-causing marine dinoflagellate *Dinophysis acuta*—Effects of light, food availability and growth phase. Harmful Algae. 2013; 23:34–45.

Papaefthimiou D, Aligizaki K, Nikolaidis G. Exploring the identity of the Greek *Dinophysis* cf. *acuminata*. Harmful Algae. 2010; 10:1–8.

Posada D, Crandall KA. Modeltest: testing the model of DNA substitution. Bioinformatics. 1998; 14:817–818. [PubMed: 9918953]

Quilliam MA, Hardstaff WR, Ishida N, McLachlan JL, Reeves AR, Ross NW, Windust AJ. Production of diarrhetic shellfish poisoning (DSP) toxins by *Prorocentrum lima* in culture and development of analytical methods. Harmful and Toxic Algal Blooms. 1996:289–292.

Raho N, Pizarro G, Escalera L, Reguera B, Marin I. Morphology, toxin composition and molecular analysis of *Dinophysis ovum* Schutt, a dinoflagellate of the "*Dinophysis acuminata* complex". Harmful Algae. 2008; 7:839–848.

Raho N, Rodríguez F, Reguera B, Marín I. Are the mitochondrial cox1 and cob genes suitable markers for species of *Dinophysis* Ehrenberg? Harmful Algae. 2013; 28:64–70.

Reguera B, Gonzalez-Gil S. Small cell and intermediate cell formation in species of *Dinophysis* (Dinophyceae, Dinophysiales). J Phycol. 2001; 37:318–333.

Reguera B, Velo-Suarez L, Raine R, Park MG. Harmful Dinophysis species: A review. Harmful Algae. 2012; 14:87–106.

Reguera B, Riobó P, Rodríguez F, Díaz P, Pizarro G, Paz B, Franco J, Blanco J. *Dinophysis* toxins: causative organisms, distribution and fate in shellfish. Mar Drugs. 2014; 12:394–461. [PubMed: 24447996]

Richlen ML, Erdner DL, McCauley LAR, Libera K, Anderson DM. Extensive genetic diversity and rapid population differentiation during blooms of *Alexandrium fundyense* (Dinophyceae) in an isolated salt pond on Cape Cod, MA, USA. Ecol Evol. 2012; 2:2588–2599. [PubMed: 23145343]

Ronquist F, Huelsenbeck JP. MrBayes 3: Bayesian phylogenetic inference under mixed models. Bioinformatics. 2003; 19:1572–1574. [PubMed: 12912839]

Rynearson TA, Newton JA, Armbrust EV. Spring bloom development, genetic variation, and population succession in the planktonic diatom *Ditylum brightwellii*. Limnol Oceanogr. 2006; 51:1249–1261.

Shankle AM, Mayali X, Franks PJS. Temporal patterns in population genetic diversity of *Prorocentrum micans* (dinophyceae). J Phycol. 2004; 40:239–247.

Smith JL, Tong M, Fux E, Anderson DM. Toxin production, retention, and extracellular release by *Dinophysis acuminata* during extended stationary phase and culture decline. Harmful Algae. 2012; 19:125–132.

Steidinger, KA. Classic taxonomy and toxic dinoflagellates. In: Ho, KC.Zhou, MJ., Qi, YZ., editors. Harmful Algae 2008, Proceedings of the 13th International Conference on Harmful Algae. ISSHA and Environmental Publication House; Hong Kong: 2009. p. 107-109.

Steidinger, KA., Tangen, K. Dinoflagellates. In: Carmelo, RT., editor. Identifying Marine Phytoplankton. Academic Press; San Diego: 1997. p. 387-584.

Suzuki T, Miyazono A, Baba K, Sugawara R, Kamiyama T. LC-MS/MS analysis of okadaic acid analogues and other lipophilic toxins in single-cell isolates of several *Dinophysis* species collected in Hokkaido, Japan. Harmful Algae. 2009; 8:233–238.

Thompson JD, Higgins DG, Gibson TJ. CLUSTAL W: improving the sensitivity of progressive multiple sequence alignment through sequence weighting, position-specific gap penalties and weight matrix choice. Nucleic Acids Res. 1994; 22:4673–4680. [PubMed: 7984417]

Tong MM, Kulis DM, Fux E, Smith JL, Hess P, Zhou QX, Anderson DM. The effects of growth phase and light intensity on toxin production by *Dinophysis acuminata* from the northeastern United States. Harmful Algae. 2011; 10:254–264.

Tong MM, Kulis DM, Jiang TJ, Qi YZ, Zhou QX, Anderson DM. Culture techniques and growth characteristics of *Dinophysis acuminata* and its prey. Chin J Oceanol Limnol. 2010; 28:1230–1239.

Trainer VL, Moore L, Bill BD, Adams NG, Harrington N, Borchert J, da Silva DAM, Eberhart BTL. Diarrhetic shellfish toxins and other polyether toxins of human health concern in Washington State. Mar Drugs. 2013; 11:1815–1835. [PubMed: 23760013]

Wilkerson FP, Grunseich G. Formation of blooms by the symbiotic ciliate *Mesodinium rubrum*: the significance of nitrogen uptake. J Plankton Res. 1990; 12:973–989.
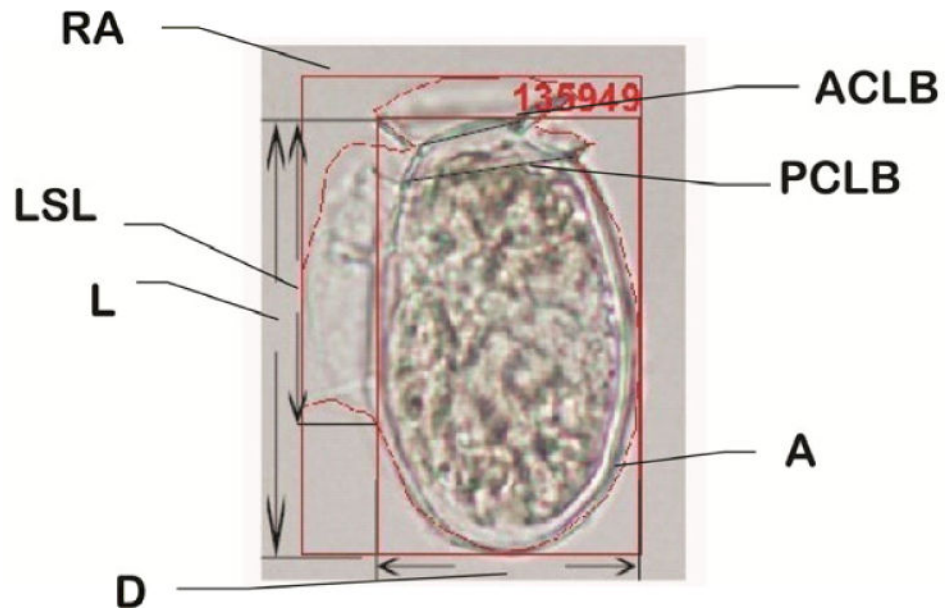
Fig.1.

Morphometric parameters of *Dinophysis* cells. Abbreviations: L: length of the body, D: depth of the body, A: area of the cells, RA: rectangular area of the cells, LSL: length of left sulcal list, ACLB: anterior cingular list width at the bottom, and PCLB: posterior cingular list width at the bottom.
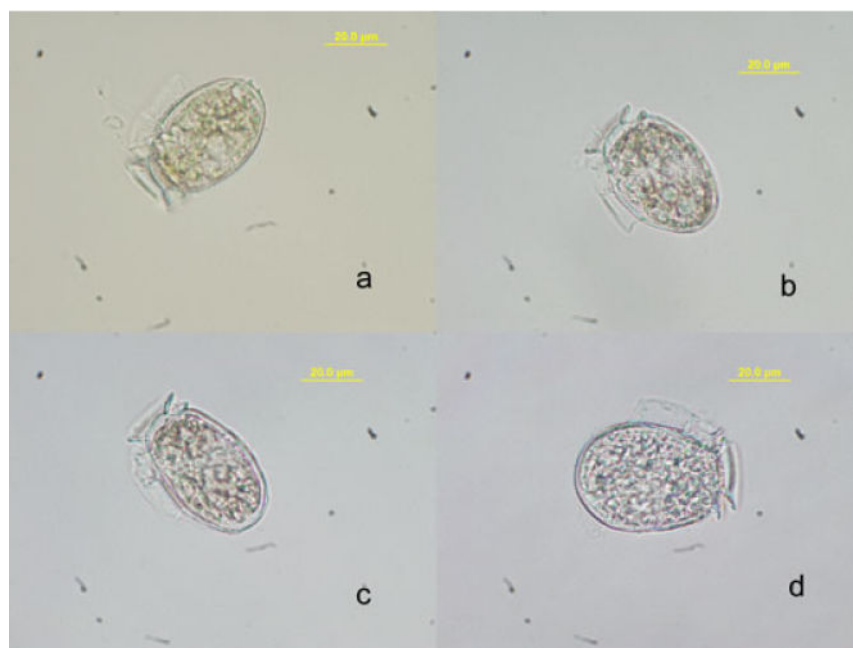
Fig.2.
Dinophysis "*acuminata*" complex. Light micrographs of cultured cells: (a) DAEP01, from Eel Pond, MA, USA; (b) DAMV01, from Martha's Vineyard, MA, USA; (c) DABOF02, from Bay of Fundy, Canada; (d) DAPA01, from Gulf of Mexico, TX, USA. Scale bars = 20 μm.
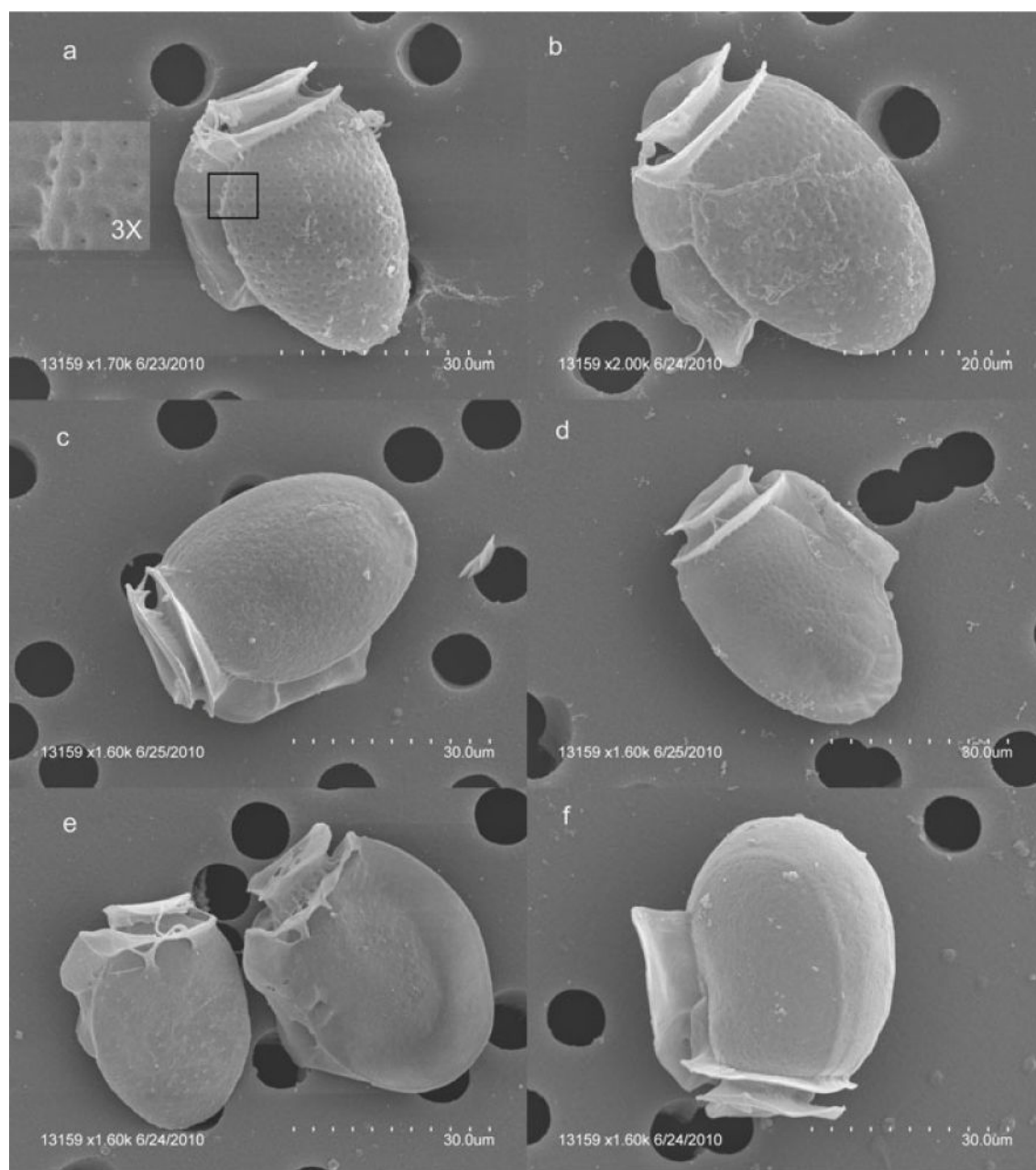
Fig. 3.
Scanning electron micrographs of preserved cultured *Dinophysis* cells. (a, b): *Dinophysis acuminata* DAEP01; (c, d): *D. acuminata* DAMV01; (e,f): *D. acuminata* DABOF02.
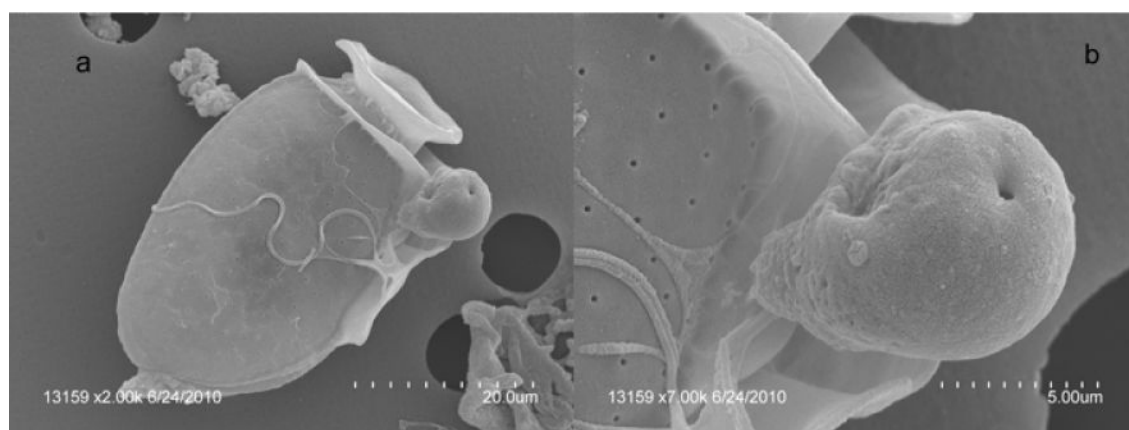
Fig. 4.
Scanning electron micrographs of preserved cultured *Dinophysis acuminata* DAEP01, with peduncle and prey residual.
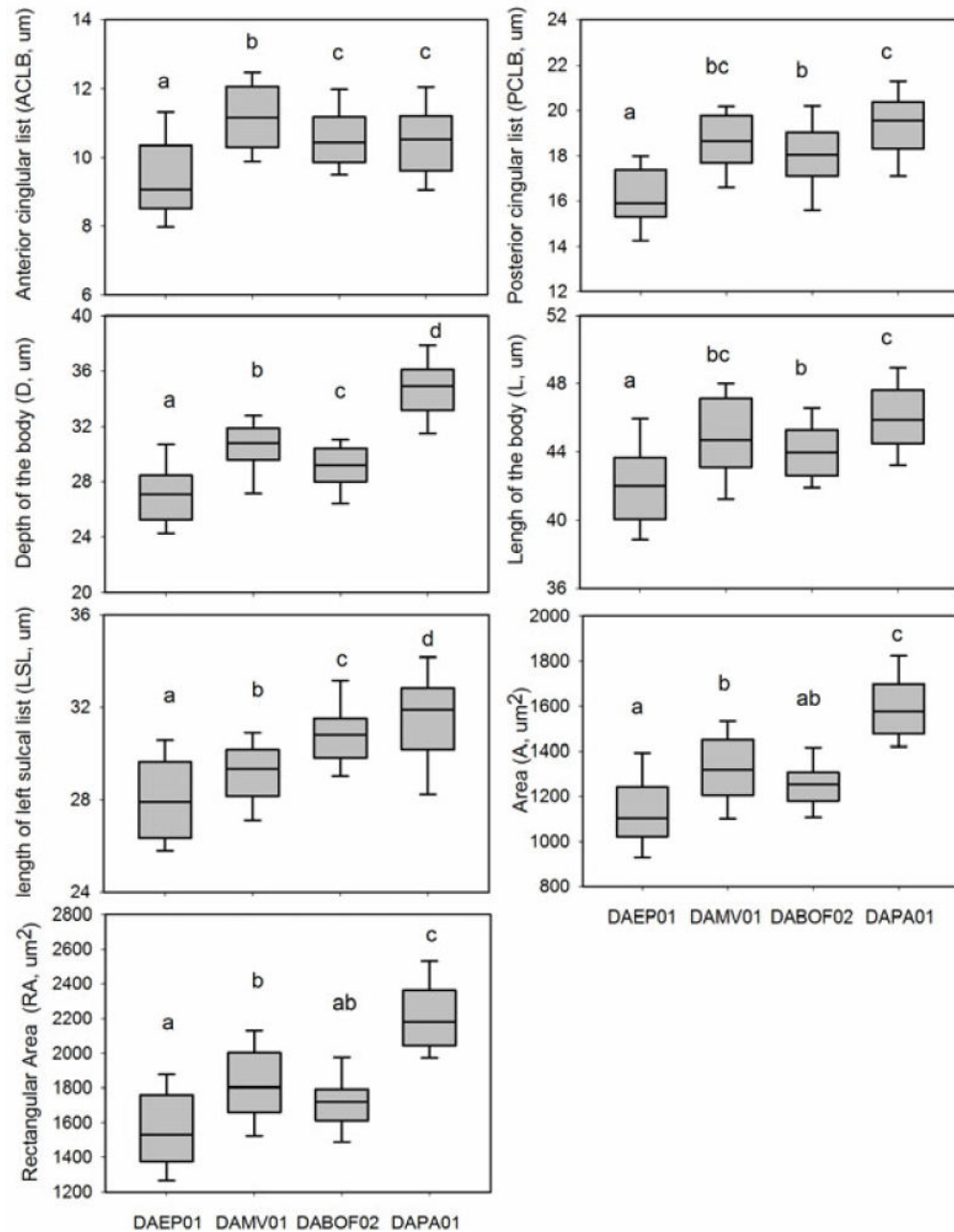
Fig. 5.
Morphometric data on anterior cingular list width at the bottom (ACLB), posterior cingular list width at the bottom (PCLB), body depth (D), body length (L), length of the sulcal list (LSL), area of the cell (A) and rectangular area of the cell (RA) of four *Dinophysis* isolates. Boxes indicate the standard error, line in box indicates the mean and the whiskers showed the min and max. Letters indicate significance (One Way ANOVA, p<0.5).
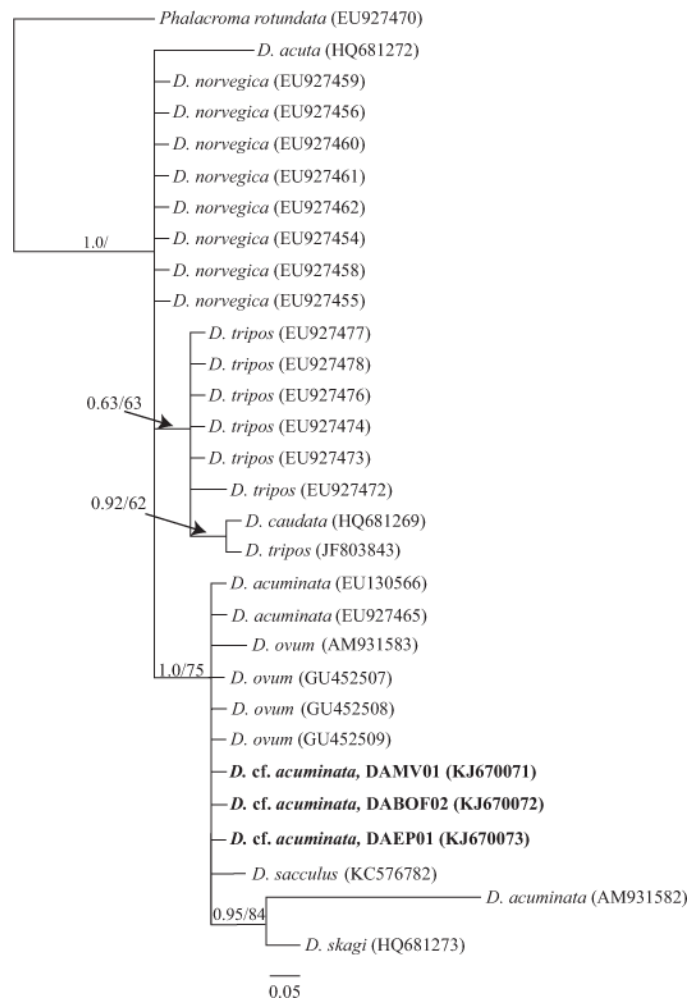
Fig. 6.

Maximum likelihood phylogenetic tree of dinoflagellates inferred from the mitochondrial *cox1*. The corresponding GenBank accession number follows the name of each organism. Names in bold represent sequences obtained in this study. Numbers at nodes are bootstrap values (1000). The scale bar represents the number of substitutions per site.
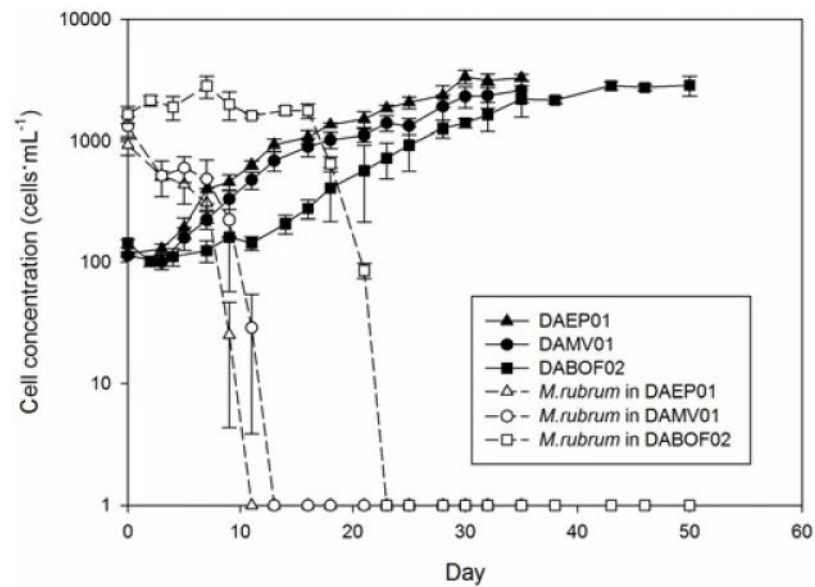
Fig. 7.

Growth response of three isolates of *D. acuminata* incubated with *M. rubrum* prey at 6°C under 65 μmol photons · m^{-2} · s^{-1}(■: DAEP01: *Dinophysis* isolate from Eel Pond, MA, USA; □: *M. rubrum* in DAEP01;●: DAMV01: *Dinophysis* isolate from Martha's Vineyard, MA, USA; ○: *M. rubrum* in DAMV01. ▲: DABOF02: *Dinophysis* isolate from Bay of Fundy, Canada; △: *M. rubrum* in DABOF02.). Mean values and standard deviations are plotted (n=3 for DAEP01 and DAMV01, n=2 for DABOF02).
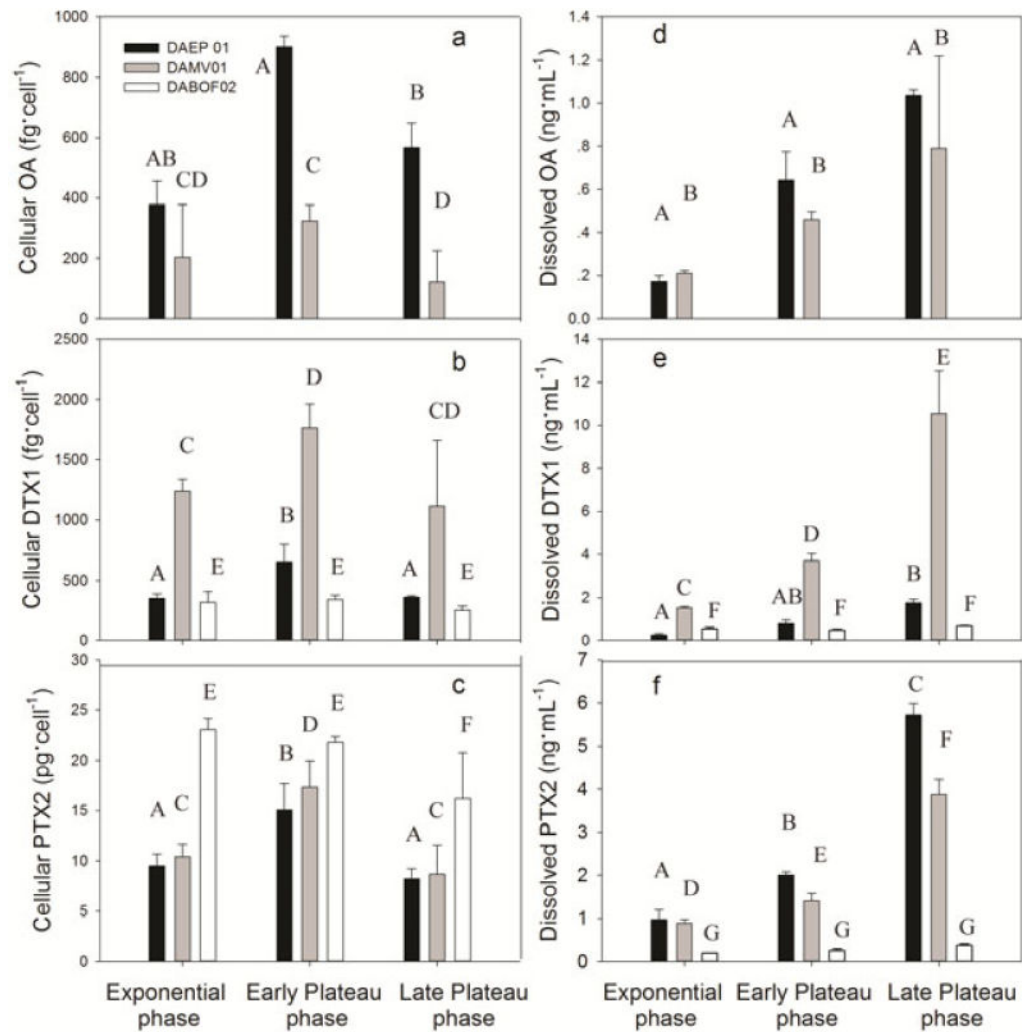
Fig. 8.
Cellular quotas and extracellular (dissolved) toxin concentrations of okadaic acid (OA, a, d), dinophysistoxin-1 (DTX1, b, e) and pectenotoxin-2 (PTX2, c, f) in three cultures of *D. acuminata* over multiple growth phases. Mean values and standard deviations are plotted (n=3 for DAEP01 and DAMV01, n=2 for DABOF02). Quotas and concentrations for each toxin were statistically analyzed for differences *within*, not between, isolates over time. Significance is indicated using dissimilar letters.

Fig. 9.
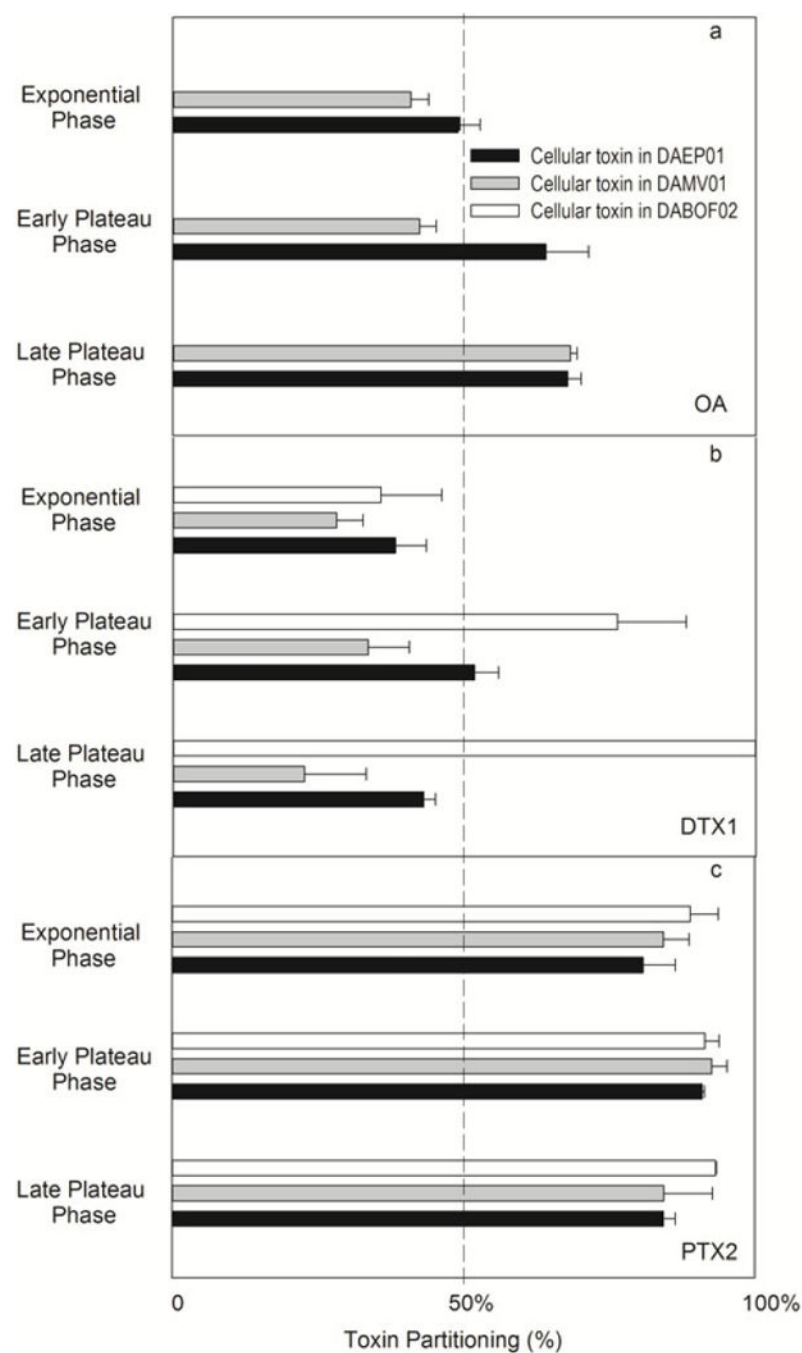Percentage of the total okadaic acid (OA), dinophysistoxin-1 (DTX1) and pectenotoxin-2 (PTX2) that was contained within the cells of *D. acuminata*, isolates DAEP01, DAMV01, and DABOF02. Percentages were calculated by dividing cellular toxin concentrations (ng per mL of culture) by total toxin concentrations (cellular + extracellular toxin concentrations, ng per mL of culture) and multiplying by 100%.

Table 1

Description of *Dinophysis* isolates.

Sample ID	Sampling site	Collection Date	Isolate type
DAEP01	Eel Pond, Woods Hole, MA, US (~41.5° N, 70.6° W)	Sep. 2006	multi-cell isolate
DAMV01	Martha's Vineyard, MA, US (~41.0° N, 70.5° W)	Aug. 2008	single cell isolate
DABOF02	Blacks Harbour, Bay of Fundy, Canada (~45.1° N, 66.8° W)	Aug. 2008	single cell isolate
DAPA01[*]	Aransas Bay, TX, US (~27.8° N, 97.1° W)	Mar. 2008	Single cell isolate

[*] This isolate was collected during a documented toxic *Dinophysis* bloom at the same location and time at that reported in Campbell et al. 2010, 27.84° N, 97.07° W, February – March 2008.

Table 2

Morphological characteristics of *Dinophysis* isolates from Northern America.

	ACLB(μm)	PCLB(μm)	D(μm)	L(μm)	LSL(μm)	A(μm²)	RA(μm²)
DAEP01	9.4±1.2	16.1±1.5	27.2±2.3	42.0±2.4	28.1±1.8	1133±152	1560±219
(n=33)	(7.8–11.9)	(13.1–19.2)	(22.8–31.3)	(37.6–47.0)	(25.7–31.5)	(905–1430)	(1256–1992)
DAMV01	11.2±1.1	18.6±1.4	30.5±2.0	44.9±2.5	29.2±1.6	1312±157	1826±213
(n=34)	(9.0–13.7)	(15.3–21.0)	(25.2–34.3)	(39.6–50.1)	(24.1–32.8)	(975–1634)	(1427–2238)
DABOF02	10.6±1.0	17.9±1.6	29.2±1.9	44.3±2.3	30.7±1.5	1260±139	1736±202
(n=40)	(8.2–12.8)	(12.9–20.6)	(25.2–34.5)	(40.8–52.1)	(26.2–33.4)	(1063–1847)	(1454–2610)
DAPA01	10.5±1.1	19.3±1.7	34.7±2.3	46.0±2.1	31.7±2.1	1594±156	2208±224
(n=43)	(7.6–12.7)	(14.0–22.6)	(29.6–39.6)	(40.7–49.9)	(27.1–36.1)	(1230–1958)	(1704–2828)

ACLB: anterior cingular list width at the bottom; PCLB: posterior cingular list width at the bottom; D: body depth; L: body length; LSL: length of the sulcal list; A: area of the cell; and RA: rectangular area of the cell.

DAEP01 is from Eel Pond, Woods Hole, MA, US; DAMV01 is from Martha's Vineyard, Massachusetts, US; DABOF02 is from Blacks Harbour, Bay of Fundy, Canada and DAPA01 is from Aransas Bay, Texas, US

Table 3

Summary of reported OA, DTX1 and PTX2 cell toxin quota in *Dinophysis acuminata* complex from different parts of the world

Species	Origin	Reference	Samples	Methods	OA	DTX1	PTX2
D. acuminata	Canada	Fux et al. 2011	Batch	LC-MS/MS	tr	p	p
D. acuminata DABOF02	Canada	Present study	Batch	LC-MS/MS	nd 0.02 pg · cell^{-1}	tr – 0.3 pg · cell^{-1} 0.2 pg · cell^{-1}	16.2 – 23.0 pg · cell^{-1} 20.4 pg · cell^{-1}
D. acuminate DAEP01	MA, USA	Hackett et al. 2009, Tong et al. 2011, present study	Batch	LC-MS/MS	0.01 – 0.1 pg · cell^{-1} 0.4–0.9 pg · cell^{-1}	0.1 – 0.3 pg · cell^{-1} 0.4–0.7 pg · cell^{-1}	8.4 – 19.2 pg · cell^{-1} 8.2–15.1 pg · cell^{-1}
D. acuminata DAMV01	MA, USA	present study	Batch	LC-MS/MS	0.1 – 0.3 pg · cell^{-1}	1.1 – 1.8 pg · cell^{-1}	8.7 – 17.3 pg cell^{-1}
D. acuminata	Japan	Kamiyama and Suzuki, 2009	Batch	LC-MS/MS	nd	2.5–4.8 pg · cell^{-1}	14.7–14.8 pg cell^{-1}
D. acuminata	Japan	Kamiyama et al. 2010	Batch	LC-MS/M	8.06–8.66 pg · cell^{-1}	0.26–0.34 pg · cell^{-1}	57.10–107.05 pg · cell^{-1}
D. acuminata	Japan	Nagai et al. 2011	Batch	LC-MS/M	2.1–12.2 pg · cell^{-1}	0.2–3.5 pg · cell^{-1}	33.8–69.9 pg · cell^{-1}
D. acuminata complex	Chile	Fux et al. 2011	Batch	LC-MS/MS	nd	nd	p
D. cf ovum DAPA01	TX, USA	Fux et al. 2011, present study	Batch	LC-MS/M	12.6 pg · cell^{-1}	nd	nd